# Multiscale Quantum Criticality Driven by Kondo Lattice Coupling in Pyrochlore Systems

Hanbit Oh, Sangjin Lee, Yong Baek Kim, and Eun-Gook Moon

Phys. Rev. Lett. **122**, 167201 — Published 24 April 2019

DOI: 10.1103/PhysRevLett.122.167201

# Multi-scale Quantum Criticality driven by Kondo-lattice Coupling in Pyrochlore Systems

Hanbit Oh[1], Sangjin Lee[1], Yong Baek Kim[2],* and Eun-Gook Moon[1]†
[1]*Department of Physics, Korea Advanced Institute of Science and Technology, Daejeon 305-701, Korea and*
[2]*Department of Physics and Centre for Quantum Materials, University of Toronto, Toronto, Ontario M5S 1A7, Canada*
(Dated: April 1, 2019)

Pyrochlore systems ($A_2B_2O_7$) with A-site rare-earth local moments and B-site 5d conduction electrons offer excellent material platforms for the discovery of exotic quantum many-body ground states. Notable examples include U(1) quantum spin liquid (QSL) of the local moments and semimetallic non-Fermi liquid of the conduction electrons. Here we investigate emergent quantum phases and their transitions driven by the Kondo-lattice coupling between such highly-entangled quantum ground states. Using the renormalization group method, it is shown that weak Kondo-lattice coupling is irrelevant, leading to a fractionalized semimetal phase with decoupled local moments and conduction electrons. Upon increasing the Kondo-lattice coupling, this phase is unstable to the formation of broken symmetry states. Particularly important is the opposing influence of the Kondo-lattice coupling and long-range Coulomb interaction. The former prefers to break the particle-hole symmetry while the latter tends to restore it. The characteristic competition leads to possibly multiple phase transitions, first from a fractionalized semimetal phase to a fractionalized Fermi surface state with particle-hole pockets, followed by the second transition to a fractionalized ferromagnetic state. Multi-scale quantum critical behaviors appear at non-zero temperatures and with external magnetic field near such quantum phase transitions. We discuss the implication of these results to the experiments on $Pr_2Ir_2O_7$.

*Introduction* : Recent advances in correlated electron systems reveal emergent phenomena beyond the Landau paradigm. Localized magnetic moments may host quantum spin liquid phases characterized by fluctuating gauge fields and fractionalized particles [1–3]. Itinerant electron systems may show non-Fermi liquid behavior without quasi-particles [4, 5]. Such phenomena and associated quantum phase transitions demand development of new concepts and novel understandings in strongly interacting quantum many body systems [6–8].

In this work, we study the intertwined model of two emergent phases beyond the Landau paradigm. We consider the interaction between the local moment system supporting a U(1) quantum spin liquid and a non-Fermi liquid semimetallic state of conduction electrons. This model is partly motivated by physics of the pyrochlore materials, $A_2B_2O_7$, where the A- and B-site pyrochlore lattices are occupied by rare-earth local moments and 5d conduction electrons, respectively. The A-site local moments may form a quantum spin liquid with emergent photons, a.k.a quantum spin ice, as suggested in $Yb_2Ti_2O_7$, $Pr_2Hf_2O_7$, and $Pr_2Zr_2O_7$ [9–17]. When the B-site is occupied by conduction electrons in 5d orbitals, such as $J_{\text{eff}}$=1/2 Kramers doublet of Ir ions, the system supports a non-Fermi liquid semimetal, so-called Luttinger-Abrikosov-Beneslaevski (LAB) state, which is derived from the quadratic band-touching with long-range Coulomb interaction [18–21]. The quadratic band-touching of Ir conduction electrons is confirmed in the ARPES experiment in the finite-temperature paramagnetic state of $Pr_2Ir_2O_7$ and $Nd_2Ir_2O_7$ [22, 23]. It is believed that the interplay between the two emergent phases mentioned above may play a crucial role in low temperature physics of $Pr_2Ir_2O_7$ [24–27] .

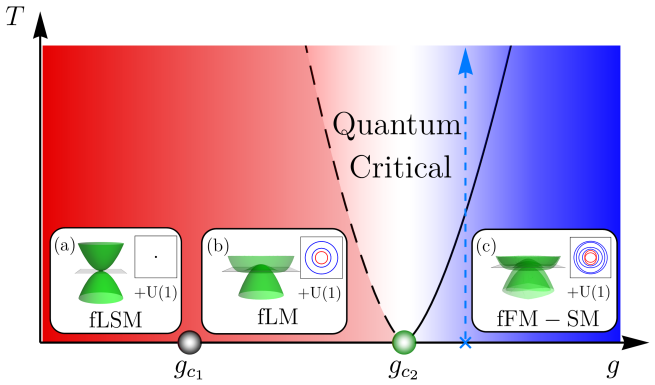


FIG. 1. Schematic phase diagram. The coupling constant $g$ characterizes strength of the Kondo-lattice coupling. The particle-hole symmetry is broken at $g_{c1}$ and the time-reversal is broken at $g_{c2}$. Insets show energy dispersions of the conducting electrons. Systems at the blue dashed line may show multi-critical behaviors with a non-zero magnetic moment at low temperatures.

Considering the Kondo-lattice coupling between the localized moments and conduction electrons, we first construct a low energy effective field theory for the coupled system of the U(1) QSL and the non-Fermi liquid semimetal state. We use the renormalization group

method to investigate emergent phases and phase transitions and find that the Kondo-lattice coupling and the long-range Coulomb interaction shows intriguing interplay physics. Namely, the former shows the tendency of breaking the particle-hole symmetry but the latter plays the opposite role. For small Kondo-lattice coupling, the Coulomb interaction prevails, and the two underlying phases remain weakly coupled. This is the Luttinger semimetal coexisting with fractionalized excitations and emergent photons from the local moments. For sufficiently strong interaction, either time-reversal or inversion symmetry may be broken and our perturbative renormalization group analysis shows that time-reversal symmetry breaking is the most relevant channel. Our analysis suggests that the particle-hole symmetry breaking occurs first as the Kondo-lattice coupling becomes dominant over the long-range Coulomb interaction, leading to a fractionalized Fermi surface state with emergent particle-hole pockets. This is followed by the time-reversal symmetry breaking transition to a ferromagnetically-ordered fractionalized semimetal phase. We discuss the resulting multi-scaling critical behavior in light of some key experiments in the low temperature phase of $Pr_2Ir_2O_7$.

*Model* : We start with a generic model Hamiltonian for the pyrochlore system, $A_2B_2O_7$,

$$\begin{aligned} H_{tot} &= H_A + H_B + H_{A-B} \\ H_A &= \sum_{\langle v,u\rangle} J_{\mu\nu}(u,v) S^\mu(u) S^\nu(v) \\ H_B &= -\sum_{\langle i,j\rangle} t_{ij}^{\alpha\beta} f_\alpha^\dagger(i) f_\beta(j) + \frac{e^2}{2}\sum_{i\neq j}\frac{n_B(i)n_B(j)}{|i-j|} \\ H_{A-B} &= \sum_{i,t} R_{\mu\nu}(v,i) S^\mu(v)\big(f_\alpha^\dagger(i)\, s_{\alpha\beta}^\nu\, f_\beta(i)\big). \end{aligned}$$

The Hamiltonian for A sites ($H_A$) describes localized magnetic moments ($S^\mu$), and the Hamiltonian for B sites ($H_B$) describes conduction electrons with annihilation and creation operators ($f_\alpha, f_\beta^\dagger$). Greek indices $(\alpha,\beta)$ are for spin quantum numbers, and $(u,v)$ and $(i,j)$ are indices for A and B sites, respectively. The Kondo-lattice coupling is described by $H_{A-B}$. A generic hopping term ($t_{ij}^{\alpha\beta}$), generic exchange interaction ($J_{\mu\nu}(u,v)$), and interaction function ($R_{\mu\nu}(u,i), s_{\alpha\beta}^\nu$) are introduced, which are constrained by lattice symmetry. The long-range Coulomb interaction with electric charge $e$ is also introduced. The local spin operators may be represented in terms of either global or local axes, $\vec{S}(u) = S^a(u)\hat{e}_a(u) = S^\mu(u)\hat{x}_\mu$. The basis vectors of the local axes ($\hat{e}_a(u)$) are commonly used in spin-ice literatures [28–32], and it is straightforward to find the relations with the basis vectors of the global axes ($\hat{x}_\mu$).

We focus on the system where spins at A sites host a U(1) QSL and electrons at B sites form the Luttinger semi-metal, motivated by the ARPES experiments [22]. The low energy effective Hamiltonian of $H_A$ may be written as the quantum spin ice Hamiltonian, $H_A \to \sum_v \frac{1}{2\mu_0}(\vec{\mathcal{B}}(v))^2 + \sum_{v^*}\frac{\epsilon_0}{2}(\vec{\mathcal{E}}(v^*))^2$ [28–30]. The "star" index, $v^*$, represents the dual diamond lattice sites of the underlying A-site pyrochlore lattice. The emergent magnetic field $\vec{\mathcal{B}}(v)$ is proportional to the average of the local spin projections to easy-axis ([111] or equivalent) directions, and the emergent electric field ($\vec{\mathcal{E}}(v^*)$) describes spin fluctuations out of local easy-axis directions. We stress that the quantum spin ice manifold is defined by the divergence-free condition, $\nabla\cdot\vec{\mathcal{B}} = 0$, and thus the $\vec{\mathcal{B}}$ fluctuations are all transversal.

The Luttinger semi-metal Hamiltonian can be approximated as $H_B(e=0) \to \sum_{\vec{k}} \Psi_k^\dagger \mathcal{H}_0(\vec{k})\Psi_k$ with a four component spinor $\Psi_k$,

$$\mathcal{H}_0(\vec{k}) = \frac{c_0}{2m}\vec{k}^2 + \frac{c_1}{2m}\sum_{n=1}^{3} d_n(\vec{k})\Gamma^n + \frac{c_2}{2m}\sum_{n=4}^{5} d_n(\vec{k})\Gamma^n.$$

At low energy, the functions $d_n(\vec{k})$ may be written as

$$\begin{aligned} &d_1(\vec{k}) = \sqrt{3}k_xk_y,\ d_2(\vec{k}) = \sqrt{3}k_xk_z,\ d_3(\vec{k}) = \sqrt{3}k_yk_z \\ &d_4(\vec{k}) = \frac{\sqrt{3}}{2}\left(k_x^2 - k_y^2\right),\ d_5(\vec{k}) = \frac{1}{2}\left(2k_z^2 - k_x^2 - k_y^2\right). \end{aligned}$$

The term with $c_0$ breaks the particle-hole symmetry (PHS), and the terms with $c_1, c_2$ are associated with the $t_{2g}$ and $e_g$ representations, respectively, of the cubic symmetry. We emphasize that the charge-neutrality of the system would demand the particle-hole band condition $|c_0| < |c_1|, |c_2|$ if there are no other electron-hole pockets far away from the zone center[22]. We also set $m = 1/2$ for simplicity unless otherwise stated. Note that the presence of the long-range Coulomb interaction makes the particle-hole and SO(3) rotational symmetries emergent in the LAB phase ($c_0 \to 0$ and $c_1 \to c_2$)[21].

The two sectors (A,B) host the excitations with fundamentally different dynamics. Namely, low energy excitations of the A-sites are emergent photons whose dispersion relation is $\omega_\lambda(\vec{q}) = v_\lambda|\vec{q}|$ with two polarizations $\lambda$ and their velocities $v_\lambda$. On the other hand, the B-sites have electronic excitations with the long-range Coulomb interaction $\epsilon(\vec{k}) \sim |\vec{k}|^z$ with $z \sim 2$.

We first construct a low energy effective coupling term of the Kondo-lattice coupling. Employing the lattice symmetries and gauge invariance, the lowest order coupling terms may be written as

$$H_{A-B} \to g\int_x \mathcal{B}_i \Psi^\dagger \hat{M}_i \Psi, \quad \hat{M}_i = \cos(\alpha)s_i + \sin(\alpha)(s_i)^3.$$

The two coupling constants ($g$ and $\alpha$) characterize the Kondo-lattice coupling. The specific form of the coupling matrix $\hat{M}$ is completely determined by the cubic and time-reversal symmetries. The 4×4 matrix ($s_i$) of a spin operator $S_i \equiv \Psi^\dagger s_i \Psi$ is used with the explicit form being introduced in SI [36]. We mainly focus on

the coupling to $\vec{\mathcal{B}}$ because $\vec{\mathcal{E}}$ couples to conduction electrons through a polarization type coupling $\hat{M}_E = \nabla$ or a Rashba type coupling $\hat{M}_E = \nabla \times \vec{s}$, which is less relevant than the coupling to $\vec{\mathcal{B}}$ (see SI [36]).

The effective low energy action of the total Hamiltonian in the Euclidean spacetime is

$$\mathcal{S}_{tot} = \mathcal{S}_A + \mathcal{S}_B + \mathcal{S}_{A-B}$$
$$\mathcal{S}_A = \int_{x,\tau} \frac{(\vec{\mathcal{B}})^2}{2\mu_0} - \frac{\epsilon_0(\vec{\mathcal{E}})^2}{2} + O((\nabla_i \mathcal{B}_j)^2, (\nabla_i \mathcal{E}_j)^2, \mathcal{E}_i^4, \mathcal{B}_j^4)$$
$$\mathcal{S}_B = \int_{x,\tau} \Psi^\dagger \left(\partial_\tau + \mathcal{H}_0(-i\nabla)\right) \Psi + \frac{e^2}{2} \int_{x,y,\tau} \frac{n(x,\tau) n(y,\tau)}{|x-y|}$$
$$\mathcal{S}_{A-B} = g \int_{x,\tau} \mathcal{B}_i \Psi^\dagger \hat{M}_i \Psi,$$

with the density operator, $n(x,\tau) = \Psi^\dagger(x,\tau)\Psi(x,\tau)$. Though the form of the Yukawa coupling with $g$ may look similar to the ones in previous literatures [33–35], we emphasize that the U(1) gauge structure in the spinice manifold plays a crucially different role here.

With a non-zero small coupling ($g \neq 0$), the dynamics of the $\mathcal{B}$ fields is modified as

$$\int_q \left(\frac{\delta_{ij}}{\mu_0}\right) \frac{\mathcal{B}_i(-q)\mathcal{B}_j(q)}{2} \;\rightarrow\; \int_q \left(\frac{\delta^{ij}}{\mu_0} + \Sigma_{\mathcal{B}}^{ij}(q)\right) \frac{\mathcal{B}_i(-q)\mathcal{B}_j(q)}{2}.$$

Hereafter, we use the four-vector notation for momentum and frequency, $k \equiv (\vec{k}, k_n)$. The boson self-energy at one-loop order is

$$\Sigma_{\mathcal{B}}^{ij}(q) = g^2 \int_{\vec{k},k_n} \mathrm{Tr}\big(\hat{\mathcal{M}}_i G_f^0(k+q) \hat{\mathcal{M}}_j G_f^0(k)\big) \quad (1)$$

with the Fermion Green's function, $G_f^0(k) = (-ik_n + \mathcal{H}_0(\vec{k}))^{-1}$. Introducing an ultraviolet (UV) cut-off $\Lambda$, we find $\Sigma_{\mathcal{B}}^{ij}(q=0) = -\delta^{ij} \frac{g^2 \Lambda}{2\pi^2}$ for the most symmetric condition ($c_1 = c_2 = 1$, $c_0 = 0$, and $\alpha = 0$), which corresponds to $\frac{1}{\mu_0} \rightarrow \frac{1}{\mu_0}(1 - \frac{\mu_0 g^2 \Lambda}{2\pi^2})$. The fermion self-energy from the gauge fluctuations is

$$\Sigma_f(k) = -g^2 \int_q \hat{M}_i \, G_f^0(k+q) \, \hat{M}_j \, \langle \mathcal{B}_i(-q) \mathcal{B}_j(+q) \rangle. \quad (2)$$

Unless $1/\mu_0 = 0$, we find the fermion self-energy,

$$\Sigma_f(k) = \mu_0 g^2 \Lambda \big(\delta c_0 \frac{\vec{k}^2}{2m} + \frac{\delta c_1}{2m} \sum_{n=1}^{5} d_n(\vec{k}) \Gamma^n\big) + \cdots \quad (3)$$

with non-zero values of $\delta c_0, \delta c_1$. For the most symmetric condition, we find $\delta c_0 = 0.025$, $\delta c_1 = -0.013$. The two self-energies are UV divergent under the Kondo-lattice coupling. The absence of logarithmic dependence on the UV cutoff means the bosonic and fermionic excitations remain weakly coupled, and the decoupled ground state ($g = 0$) is stable as far as the Kondo-lattice coupling is small. We call this state the fractionalized Luttinger semi-metal (fLSM).

We stress that the Kondo-lattice coupling generates the PHS breaking term as manifested by $\delta c_0 \neq 0$ even with the most symmetric bare Hamiltonian ($c_0 = 0$). This contribution arises from the transversal gauge fluctuations, and the absence of the longitudinal gauge fluctuations is essential. The competition between the Kondo-lattice coupling and the long-range Coulomb interaction plays an important role in the PHS channel of fLSM. In the perturbative regime $\mu_0 g^2 \Lambda \ll 1$, the long-range Coulomb interaction is more relevant than the Kondo-lattice coupling [21], and the PHS is realized.

Adjacent phases of fLSM may be obtained by using the lattice symmetries. Considering time-reversal symmetry and parity as well as the rotational symmetries, a ground state with $\langle \mathcal{B}_i \rangle \neq 0$ breaks time-reversal symmetry and rotations but not parity. The resulting time-reversal broken phase hosts nodal conduction electrons in the form of Weyl semi-metals or metals. We call such a semi-metal phase with broken time-reversal symmetry a fractionalized ferromagnetic semi-metal (fFM-SM). The presence of both gapless electronic and gauge excitations is one of the main characteristics of fFM-SM, different from other states such as the Coulombic ferromagnetic state [31]. Similarly, a state with $\langle \mathcal{E}_i \rangle \neq 0$ and $\langle \mathcal{B}_i \rangle = 0$ is naturally dubbed a fractionalized ferroelectric phase, and one with $\langle \mathcal{E}_i \rangle, \langle \mathcal{B}_i \rangle \neq 0$ may be called a fractionalized multiferroic phase. As shown below, however, there may exist another transition before the system reaches the fFM-SM.

*Quantum Phase Transitions* : To investigate transitions to symmetry-broken phases, we first extend and apply Landau's mean field analysis, which amounts to ignoring spatial and temporal fluctuations of the emergent fields via $\mathcal{B}_i(x,\tau) \rightarrow \mathcal{B}_i$. Integrating out the fermion excitations, we obtain the effective action of $\mathcal{B}_i$, and a continuous quantum phase transition between fLSM and fFM-SM is obtained for $g > g_c$ (similar to the one of [34], and also see SI [36]). At the one-loop level, we find $g_c = \sqrt{2\pi^2/(\mu_0 \Lambda)}$ for the most symmetric condition. The continuous transition obtained in the mean-field calculation respects the PHS and $SO(3)$ rotational symmetry because fLSM enjoys those symmetries.

We, however, show that the gauge fluctuations destabilize the continuous transition of the mean-field calculation. Defining $\delta\Sigma_{\mathcal{B}}^{ij}(q) = \Sigma_{\mathcal{B}}^{ij}(q) - \Sigma_{\mathcal{B}}^{ij}(0)$, we find that the boson self-energy has the form,

$$\delta\Sigma_{\mathcal{B}}^{ij}(q) = g^2 \Big(a_T |\vec{q}| + a_\omega \sqrt{|q_n|}\Big) (\delta^{ij} - \frac{q^i q^j}{\vec{q}^2}).$$

The condition $\nabla \cdot \mathcal{B} = 0$ enforces that the fluctuations are transversal, and the dimensionless functions $(a_T, a_\omega)$ are positive in a wide range of the parameters which are illustrated in SI. Their positiveness indicates that the gauge fluctuations are stable with the renormalized propagator $\big(\Sigma_{\mathcal{B}}^{ij}(q)\big)^{-1}$.

Let us assume that there is a stable continuous tran-

sition between fLSM and fFM-SM. At the critical point ($g = g_c$), the dominant boson propagator may be written as

$$\langle \mathcal{B}_i(-q)\mathcal{B}_j(+q)\rangle = \frac{1}{g_c^2}\frac{1}{a^T|\vec{q}| + a_\omega\sqrt{|q_n|}}(\delta^{ij} - \hat{q}^i\hat{q}^j) \quad (4)$$

omitting higher order terms. To control calculations better, one may introduce the flavor number of fermions ($N_f$) and perform $1/N_f$ calculations (see SI [36]). The PHS breaking term can be obtained by evaluating

$$\frac{\partial \mathrm{Tr}\big[\Sigma_f(k)\big]}{\partial \vec{k}^2} = -\int_q \frac{\partial}{\partial \vec{k}^2}\frac{\mathrm{Tr}\big[G_f^0(k+q)(\hat{M}_i\hat{M}_i - \hat{M}_i\hat{M}_j\hat{q}^i\hat{q}^j)\big]}{a^T|\vec{q}| + a_\omega\sqrt{|q_n|}}.$$

The integral is logarithmically divergent,

$$\Lambda\frac{\partial}{\partial\Lambda}\Big(\frac{\partial \mathrm{Tr}\big[\Sigma_f(k)\big]}{\partial \vec{k}^2}\Big) = 4\delta_0. \quad (5)$$

Including both the gauge-fluctuations and the long-range Coulomb interaction, we find $\delta_0 \neq 0$ ($\delta_0 = 0.3601$ for the most symmetric condition), which can be interpreted as a divergent $\delta c_0$. The logarithmic divergence demonstrates the PHS cannot be realized at the critical point, which indicates the Kondo-lattice coupling dominates the long-range Coulomb interaction near the critical point. Thus, there is no continuous quantum phase transition between fLSM and fFM-SM.

The divergence of the PHS breaking term destabilizes not only the validity of the mean-field calculation but also the particle-hole band condition ($|c_0| < |c_1|, |c_2|$). We find that the corrections of $c_{1,2}$ are smaller than the one of $c_0$, and thus the particle-hole symmetry condition may break down at long wave-length and low energy. The charge neutrality condition then enforces the formation of electron and hole pockets near the Brillouin zone center.

We propose, based on the above calculations, that the PHS is broken before the onset of $\langle \mathcal{B}_i\rangle$, whose validity is self-consistently checked a posteriori. The transition between fLSM and fFM-SM is intervened by an intermediate phase with the electron and hole pockets dubbed the fractionalized Luttinger metal (fLM). There *must* be more than one continuous transition between fLSM and fFM-SM as illustrated in Fig. 1. The transition between fLSM and fLM is likely to be described by the Lifshitz transition. Once the pockets appear, the scale ($\epsilon_F \neq 0$) associated with the size of the Fermi pockets is emergent. The long-range Coulomb interaction is screened by the Thomas-Fermi screening, and the Yukawa coupling induces the Landau damping term similar to the one of the Hertz-Millis theory. Thus, in spite of the presence of the gauge structure, the critical theory becomes

$$\mathcal{S}_H = \int_q (r + \gamma\frac{|q_n|}{|\vec{q}|} + |\vec{q}|^2)|\mathcal{B}_i(q)|^2 + \frac{u}{4}\int_{x,\tau}(\mathcal{B}_i)^4 - h^i_{ext}\mathcal{B}_i.$$

The term with $\gamma = \gamma(\epsilon_F)$ is for the Landau-damping, and the coefficient of the term with $|\vec{q}|^2$ is normalized to be one. We omit the term with $\mathcal{E}_i^2$ because it is irrelevant at the critical point (say, $r = 0$). Namely, the dynamics of the gauge fluctuations are determined by the damping term, and the critical modes have the dynamical critical exponent $z_H = 3$. Since $d + z_H > 4$, the term $(\mathcal{B}_i)^4$ with $u$ is irrelevant, and the gauge fluctuations are weakly correlated with $z_H = 3$. The operator scaling dimensions are $[\mathcal{B}_i(x,\tau)] = 2$, $[r] = 2$, and $[h^i_{ext}] \equiv \nu^{-1}_{ext} = 4$.

*Multi-scale Quantum Criticality* : The interplay between the Kondo-lattice coupling and the long-range Coulomb interaction naturally brings about multi-scale quantum criticality around the onset of $\langle B_i\rangle$. To see this, let us estimate the energy scale for breaking the particle-hole band condition by using Eqn. (5). Setting $\Lambda\frac{d}{d\Lambda} \equiv \frac{d}{dl}$, the renormalization group equation is $\frac{d}{dl}c_0 \simeq 0.3601$, and the assumption $c_0 < c_1$ becomes invalid at $l^* \sim 3$. The associated energy scale is $E_{IR} \sim \Lambda^2\, e^{-2l^*} \sim \Lambda^2/400$ with the UV cutoff scale, $\Lambda$, below which the assumption of small $c_0$ breaks down. The energy scale $E_{IR}$ is much smaller than the band-width of the conduction electron, which is of the order $\sim \Lambda^2$. It is natural to expect that the emergent particle-hole pocket-size scale ($\epsilon_F$) in the intermediate phase between fLSM and fFM-SM is of similar order of magnitude, namely $E_{IR} \sim \epsilon_F$.

Because of the hierarchy of energy scales, three sets of critical exponents would naturally appear in physical quantities near the onset of $\langle B_i\rangle$. For example, the emergent photons have $z_1 = 1$, the non-Fermi liquid excitations have $z_2 \sim 2$, and the Hertz-Millis fluctuations have $z_3 = 3$. The scaling dimensions of the external magnetic field are easily obtained by considering the coupling to the magnetic field. The emergent magnetic field couples to the Zeeman external magnetic field via $\int_{x,\tau}\vec{\mathcal{B}}\cdot\vec{h}_{ext}$, and the scaling dimension of the external field is $\nu^{-1}_{ext,1} = 2$. The conduction electron couples to the external field as $\int_{x,\tau}\psi^\dagger M\psi\cdot\vec{h}_{ext}$, which gives $\nu^{-1}_{ext,2} \sim 2$. We also show that the Hertz-Millis type fluctuation gives $\nu^{-1}_{ext,3} = 4$.

Three different scaling behaviors can naturally arise in all physical quantities. For example, the magnetic Gruneissen parameter, $\Gamma_H = -(\partial M/\partial T)_H/c_H$ with magnetization ($M$) and specific heat ($c_H$) at constant external magnetic field $H$, has the scaling form,

$$\Gamma_H = \frac{1}{h_{ext}}\mathcal{F}\Big(\frac{T^{1/(z_1\nu_{ext,1})}}{h_{ext}}, \frac{T^{1/(z_2\nu_{ext,2})}}{h_{ext}}, \frac{T^{1/(z_3\nu_{ext,3})}}{h_{ext}}; \frac{T}{E_{IR}}\Big).$$

The dimensionless function, $\mathcal{F}$, manifests the multi-scale quantum criticality. For example, when $T \gg E_{IR}$, one can find $\mathcal{F}(x,y,z;0) = b_0 + b_1x + b_2y + b_3z$ with three coefficients $b_{0,1,2,3}$ for $x, y, z \ll 1$.

Possible exponents are $z_1\nu_{ext,1} = 1/2$ for the emergent photons and $z_2\nu_{ext,2} = 1 + O(1/N_f)$ for conduction electrons in fLSM. Most importantly, near the quantum phase transition to the fractionalized ferromagnetic semimetal state, the Hertz-Millis QCP gives the scaling expo-

nent, $z_3\nu_{ext,3} = 3/4$. It is interesting to note that similar multi-scaling critical behavior in magnetic Gruneisen parameter is seen in $Pr_2Ir_2O_7$ [27]. Our theory naturally explains the appearance of Fermi-pockets at low temperatures with multi-scaling behaviors even though the calculated critical exponents are not exactly the same as the experimentally-determined value.

We also remark that our theory allows two channels, semi-metallic conduction electrons and collective modes of the U(1) QSL, to contribute to magnetic susceptibility and other thermodynamic quantities. An interesting question is whether the contributions of such unusual excitations to thermodynamic and transport properties can explain various non-Fermi liquid behaviors seen in the experiment on $Pr_2Ir_2O_7$. We leave this intriguing problem for a future work.

In conclusion, we investigate emergent quantum phenomena arising from the Kondo-lattice coupling between the quantum spin liquid of local moments and non-Fermi liquid conduction electrons in pyrochlore systems $A_2B_2O_7$. Intertwined actions between the Kondo-lattice coupling and the long-range Coulomb interaction are uncovered. As an important result, quantum criticality near the onset of ferromagnetic ordering naturally displays multi-scaling behaviors. Further works on more quantitative analysis and comparison with experiments are highly desired.

This work was supported by NRF of Korea under Grant No. 2017R1C1B2009176 (HO, SL, EGM), and the NSERC of Canada, CIFAR, and Center for Quantum Materials at the University of Toronto (YBK). This work was performed in part at the Aspen Center for Physics, which is supported by National Science Foundation grant PHY-1607611 (YBK). EGM also acknowledges the support of the POSCO Science Fellowship of POSCO TJ Park Foundation.

* ybkim@physics.toronto.ca
† egmoon@kaist.ac.kr

[1] M. J. P. Gingras and P. A. McClarty, Reports on Progress in Physics **77**, 056501 (2014).
[2] L. Savary and L. Balents, Reports on Progress in Physics **80**, 016502 (2017).
[3] Y. Zhou, K. Kanoda, and T.-K. Ng, Rev. Mod. Phys. **89**, 025003 (2017).
[4] A. J. Schofield, Contemporary Physics **40**, 95 (1999).
[5] S.-S. Lee, Annual Review of Condensed Matter Physics **9**, 227 (2018).
[6] T. Senthil, A. Vishwanath, L. Balents, S. Sachdev, and M. P. A. Fisher, Science **303**, 1490 (2004).
[7] X.-G. Wen, Rev. Mod. Phys. **89**, 041004 (2017).
[8] W. Witczak-Krempa, G. Chen, Y. B. Kim, and L. Balents, Annual Review of Condensed Matter Physics **5**, 57 (2014).
[9] K. Kimura, S. Nakatsuji, J.-J. Wen, C. Broholm, M. B. Stone, E. Nishibori, and H. Sawa, Nature Communications **4**, 1934 EP (2013).
[10] M. Hirschberger, J. W. Krizan, R. J. Cava, and N. P. Ong, Science **348**, 106 (2015).
[11] K. A. Ross, L. Savary, B. D. Gaulin, and L. Balents, Phys. Rev. X **1**, 021002 (2011).
[12] Y. Tokiwa, T. Yamashita, M. Udagawa, S. Kittaka, T. Sakakibara, D. Terazawa, Y. Shimoyama, T. Terashima, Y. Yasui, T. Shibauchi, and Y. Matsuda, Nature Communications **7**, 10807 EP (2016).
[13] L. Pan, N. J. Laurita, K. A. Ross, B. D. Gaulin, and N. P. Armitage, Nature Physics **12**, 361 EP (2015), article.
[14] S. Erfanifam, S. Zherlitsyn, S. Yasin, Y. Skourski, J. Wosnitza, A. A. Zvyagin, P. McClarty, R. Moessner, G. Balakrishnan, and O. A. Petrenko, Phys. Rev. B **90**, 064409 (2014).
[15] V. K. Anand, L. Opherden, J. Xu, D. T. Adroja, A. T. M. N. Islam, T. Herrmannsdörfer, J. Hornung, R. Schönemann, M. Uhlarz, H. C. Walker, N. Casati, and B. Lake, Phys. Rev. B **94**, 144415 (2016).
[16] J. D. Thompson, P. A. McClarty, D. Prabhakaran, I. Cabrera, T. Guidi, and R. Coldea, Phys. Rev. Lett. **119**, 057203 (2017).
[17] Y. Tokiwa, T. Yamashita, D. Terazawa, K. Kimura, Y. Kasahara, T. Onishi, Y. Kato, M. Halim, P. Gegenwart, T. Shibauchi, S. Nakatsuji, E.-G. Moon, and Y. Matsuda, Journal of the Physical Society of Japan **87**, 064702 (2018).
[18] J. M. Luttinger, Phys. Rev. **102**, 1030 (1956).
[19] A. Abrikosov, L. Gorkov, and I. Dzyaloshinskii, Sov. Phys. JETP **9**, 636 (1959).
[20] A. Abrikosov, J. Exp. Theor. Phys **66**, 1443 (1974).
[21] E.-G. Moon, C. Xu, Y. B. Kim, and L. Balents, Phys. Rev. Lett. **111**, 206401 (2013).
[22] T. Kondo, M. Nakayama, R. Chen, J. J. Ishikawa, E.-G. Moon, T. Yamamoto, Y. Ota, W. Malaeb, H. Kanai, Y. Nakashima, Y. Ishida, R. Yoshida, H. Yamamoto, M. Matsunami, S. Kimura, N. Inami, K. Ono, H. Kumigashira, S. Nakatsuji, L. Balents, and S. Shin, Nature Communications **6**, 10042 EP (2015).
[23] M. Nakayama, T. Kondo, Z. Tian, J. J. Ishikawa, M. Halim, C. Bareille, W. Malaeb, K. Kuroda, T. Tomita, S. Ideta, K. Tanaka, M. Matsunami, S. Kimura, N. Inami, K. Ono, H. Kumigashira, L. Balents, S. Nakatsuji, and S. Shin, Phys. Rev. Lett. **117**, 056403 (2016).
[24] B. Cheng, T. Ohtsuki, D. Chaudhuri, S. Nakatsuji, M. Lippmaa, and N. P. Armitage, Nature Communications **8**, 2097 (2017).
[25] S. Nakatsuji, Y. Machida, Y. Maeno, T. Tayama, T. Sakakibara, J. v. Duijn, L. Balicas, J. N. Millican, R. T. Macaluso, and J. Y. Chan, Phys. Rev. Lett. **96**, 087204 (2006).
[26] Y. Machida, S. Nakatsuji, S. Onoda, T. Tayama, and T. Sakakibara, Nature **463**, 210 EP (2009).
[27] Y. Tokiwa, J. J. Ishikawa, S. Nakatsuji, and P. Gegenwart, Nature Materials **13**, 356 EP (2014), article.
[28] A. Banerjee, S. V. Isakov, K. Damle, and Y. B. Kim, Phys. Rev. Lett. **100**, 047208 (2008).
[29] M. Hermele, M. P. A. Fisher, and L. Balents, Phys. Rev. B **69**, 064404 (2004).
[30] O. Benton, O. Sikora, and N. Shannon, Phys. Rev. B **86**, 075154 (2012).
[31] L. Savary and L. Balents, Phys. Rev. Lett. **108**, 037202

(2012).
[32] S. Lee, S. Onoda, and L. Balents, Phys. Rev. B **86**, 104412 (2012).
[33] L. Savary, E.-G. Moon, and L. Balents, Phys. Rev. X **4**, 041027 (2014).
[34] J. M. Murray, O. Vafek, and L. Balents, Phys. Rev. B **92**, 035137 (2015).
[35] X.-P. Yao and G. Chen, Phys. Rev. X **8**, 041039 (2018).
[36] See Supplemental Information [url] for the details of the notations, the construction of Yukawa couplings between fermions and emergent gauge fields, the stability check of the guage fluctuation near the QCP, large $N_f$ calculations, which includes Refs.[27, 34, 37] .
[37] S. Murakami, N. Nagosa, and S.-C. Zhang, Phys. Rev. B **69**, 235206 (2004).